

## Electronic Supporting Information

### A unique 3D ultramicroporous triptycene-based polyimide framework for efficient gas sorption applications

Bader Ghanem,<sup>a</sup> Youssef Belmabkhout,<sup>a</sup> Yingge Wang,<sup>a</sup> Yunfeng Zhao,<sup>a</sup> Yu Han,<sup>a</sup> Mohamed Eddaoudi,<sup>a</sup> Ingo Pinnau<sup>a\*</sup>

*Advanced Membranes and Porous Materials Center,  
Physical Sciences and Engineering Division, King Abdullah University of Science and  
Technology (KAUST), Al-Jazri Building, Thuwal 23955-6900, KSA.*

Corresponding author Email: [ingo.pinnau@kaust.edu.sa](mailto:ingo.pinnau@kaust.edu.sa)

#### Contents

#### Figures, Tables, and Schemes

**Fig. S1** FT-IR spectrum of the trisphthalonitrile **2**.

**Fig. S2** FT-IR spectrum of the trisanhydride monomer **3**.

**Fig. S3** <sup>1</sup>H NMR spectrum of the trisphthalonitrile **2** in DMSO-*d*<sub>6</sub>.

**Fig. S4** <sup>1</sup>H NMR spectrum of the trisanhydride monomer **3** in CDCl<sub>3</sub>.

**Fig. S5** TGA trace of TTAPI network.

**Fig. S6** Powder XRD pattern for TTAPI network polymer.

**Fig. S7** Pore size distributions of TTAPI determined from CO<sub>2</sub> sorption at 273 K.

h pressure absolute and excess H<sub>2</sub> uptake of TTAPI network at 77 K.

**Fig. S9** Heat of sorption curves calculated for CO<sub>2</sub> and H<sub>2</sub> sorption on TTAPI network.

**Fig. S10** IAST predictions of CO<sub>2</sub>/N<sub>2</sub> selectivity (15% CO<sub>2</sub> and 85% N<sub>2</sub>) for TTAPI network.

**Fig. S11** High pressure CO<sub>2</sub> and CH<sub>4</sub> uptake of TTAPI network at 298 K.

**Table S1.** Properties of various porous materials and their gas adsorption performance.

**Image S1:** Representation of the Rubotherm gravimetric-densimetric apparatus.

#### Experimental Section

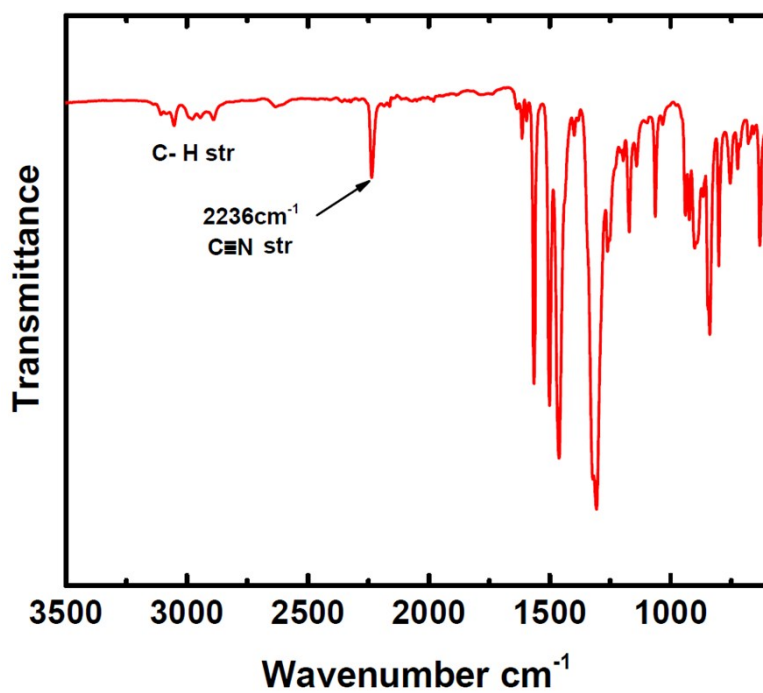


Fig. S1  
spectrum

of the  
trisphthalonitrile monomer 2.

FT-IR  
of the

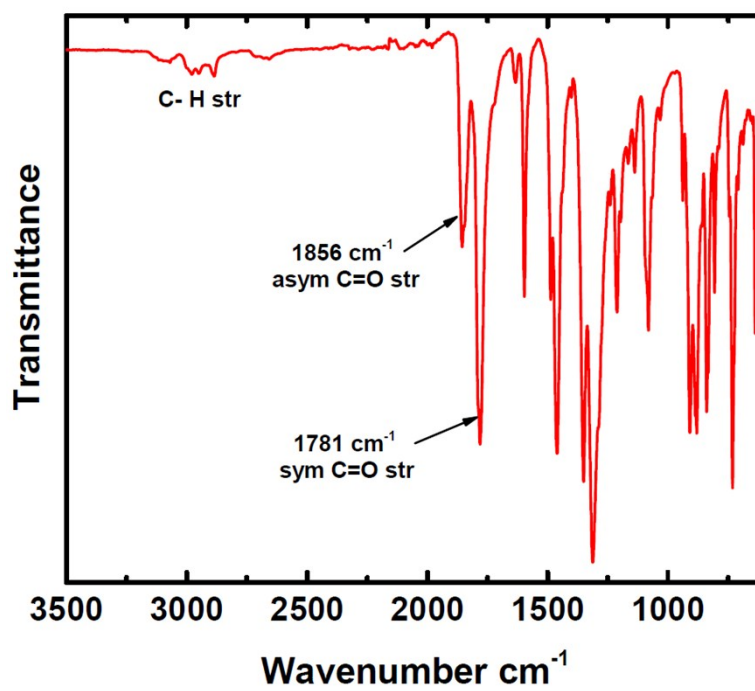
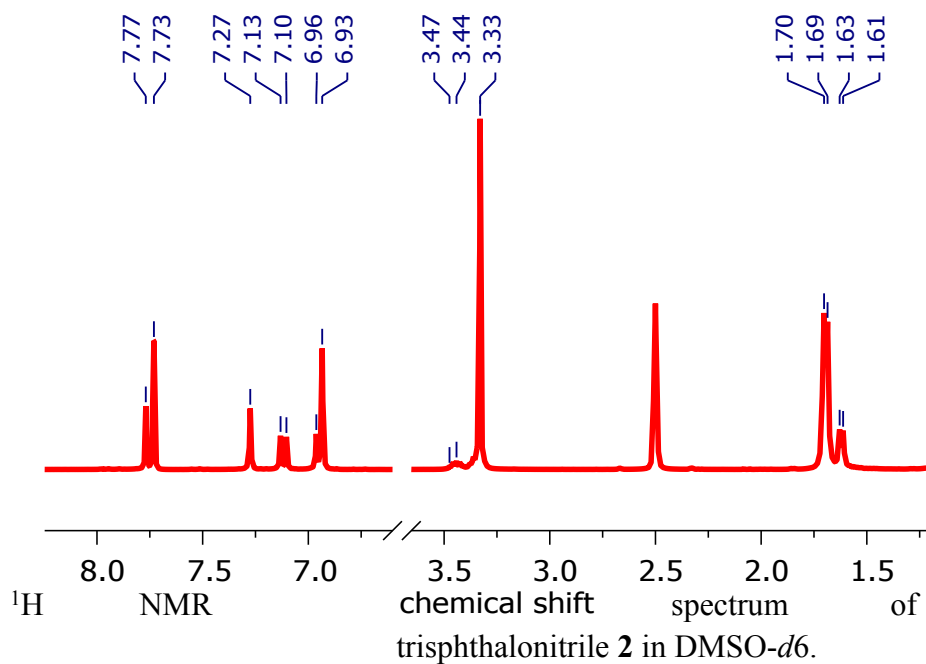


Fig. S2 FT-IR spectrum of the trisanhydride monomer 3.



S3

the

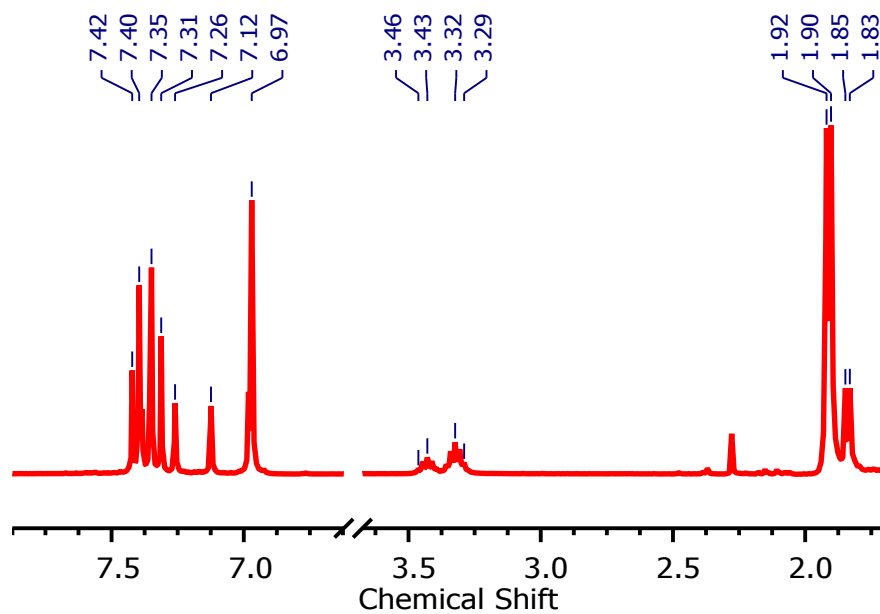
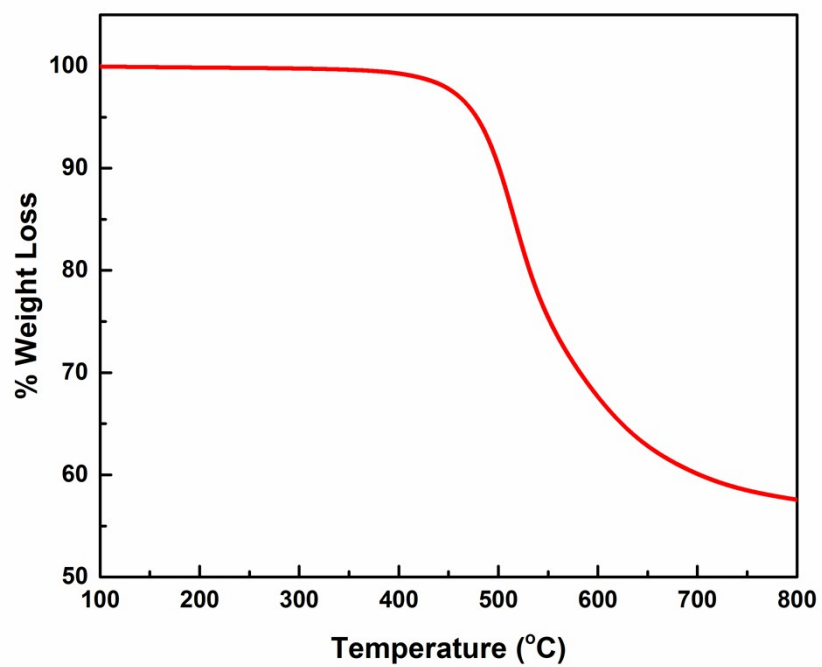


Fig.

S4  $^1\text{H}$

NMR spectrum of the trisanhydride monomer **3** in  $\text{CDCl}_3$ .



**Fig. S5** TGA trace of TTAPI network.

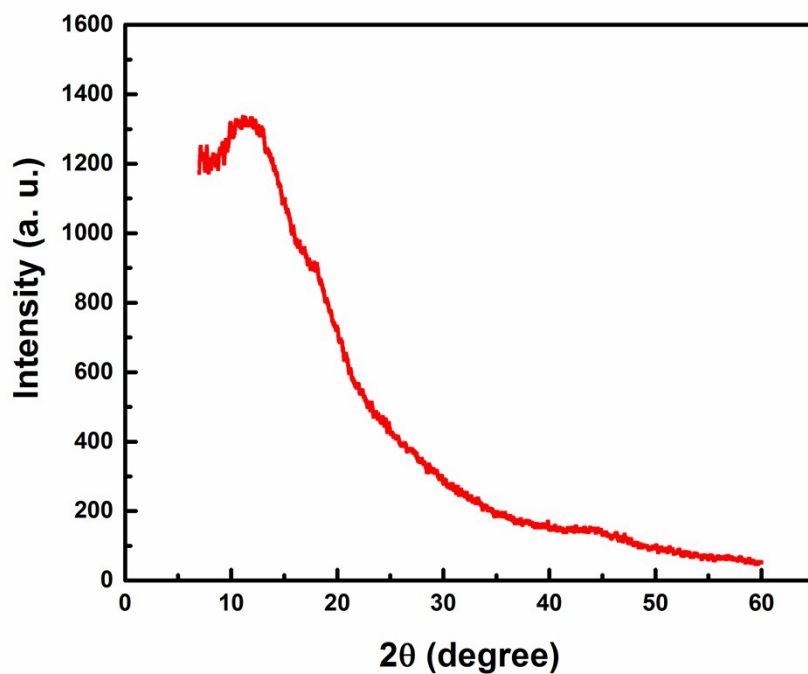


**Fig. S6** Powder XRD pattern for TTAPI network polymer.

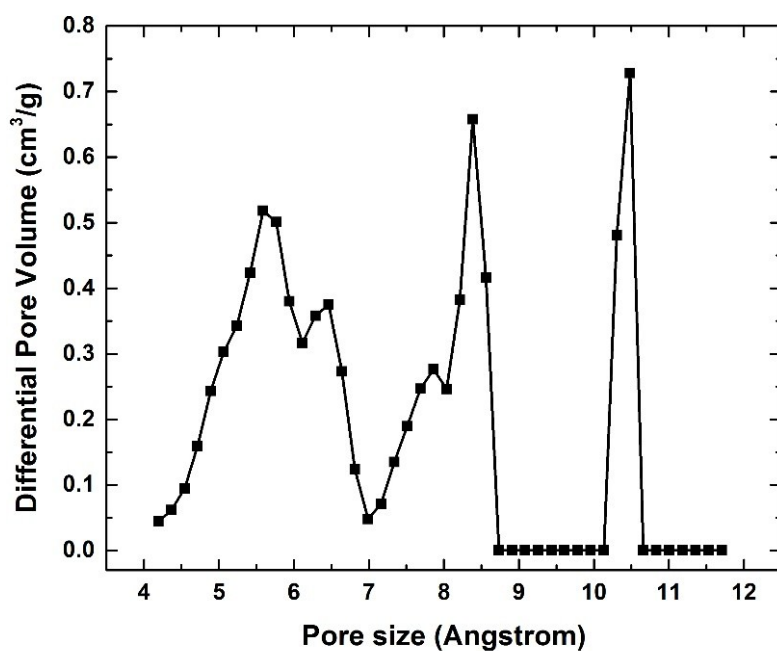


Fig. S7 Pore size distributions of TTAPI determined from CO<sub>2</sub> sorption at 273 K.

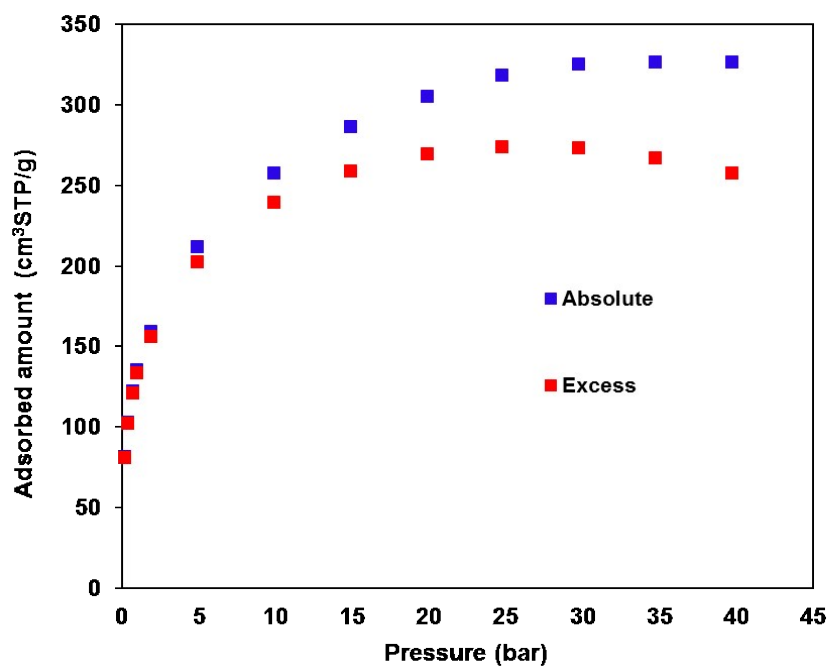
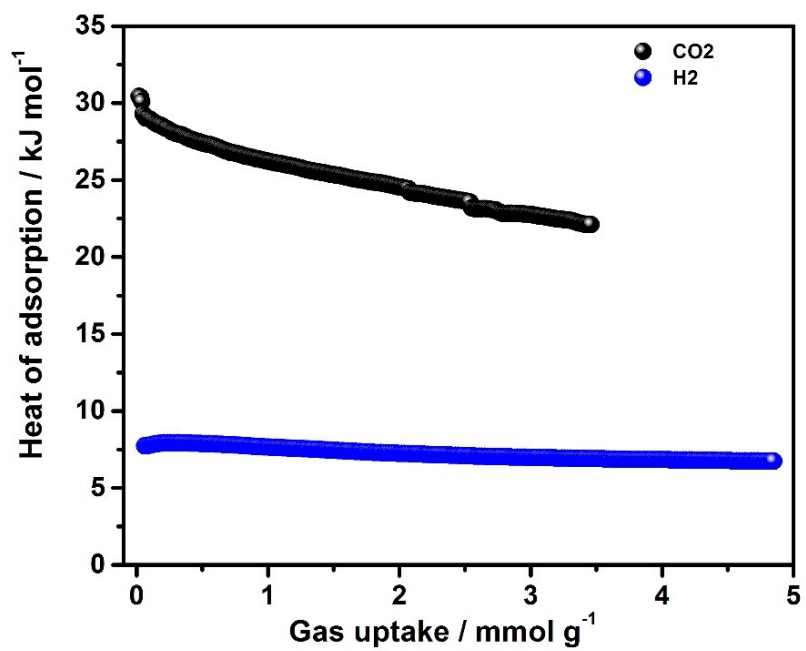
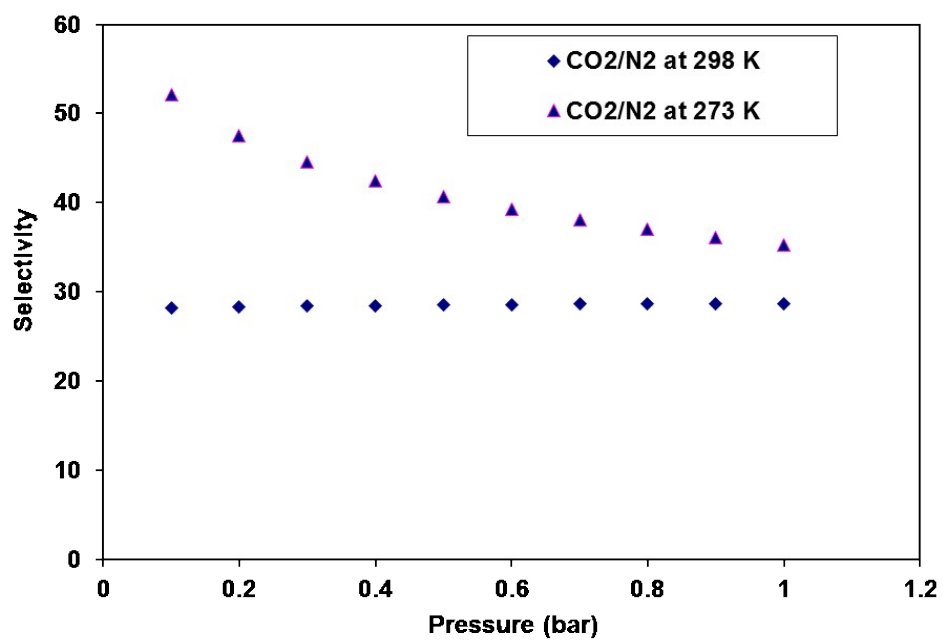


Fig. S8 High-pressure absolute and excess H<sub>2</sub> uptake of TTAPI network at 77 K.



**Fig. S9** Heat of sorption curves calculated for CO<sub>2</sub> and H<sub>2</sub> sorption on TTAPI network.



**Fig. S10** IAST predictions of CO<sub>2</sub>/N<sub>2</sub> selectivity (15% CO<sub>2</sub> and 85% N<sub>2</sub>) for TTAPI network.

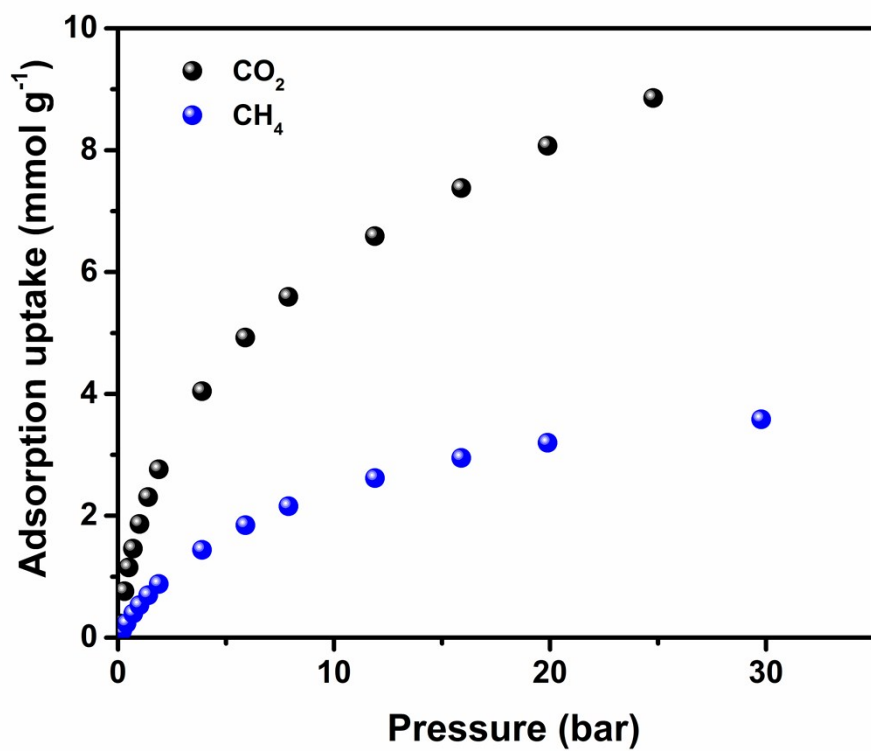


Fig. S11 High-pressure CO<sub>2</sub> and CH<sub>4</sub> uptake of TTAPI network at 298 K.

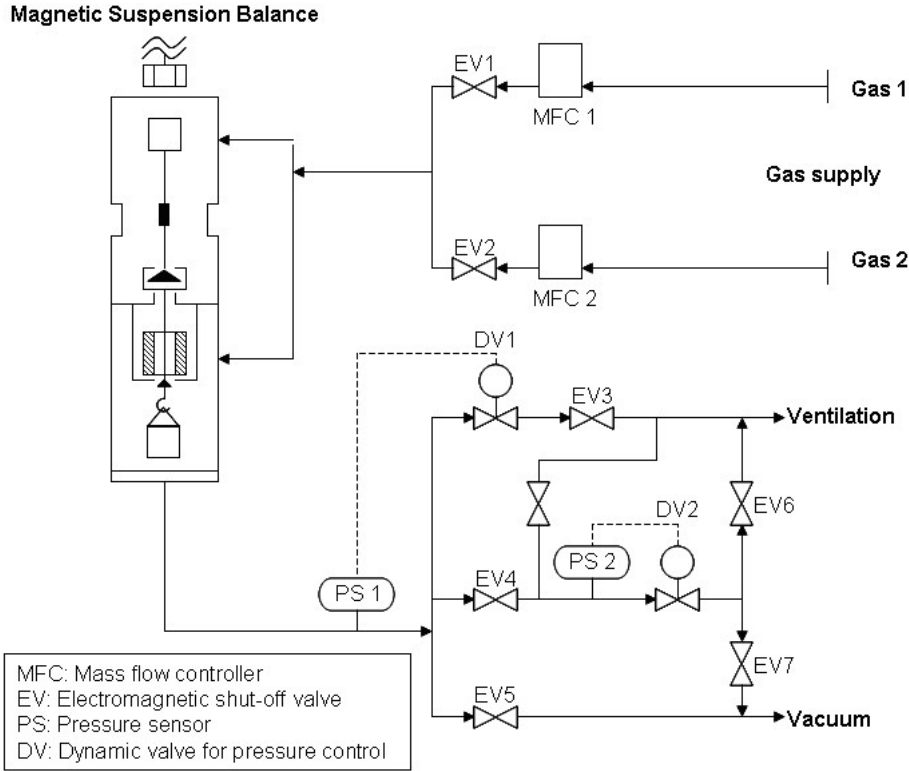
Table S1. Properties of various porous materials and their gas sorption performances

Type of Porous Materials	BET SA (m <sup>2</sup> /g)	CO <sub>2</sub> Uptake (mmol/g)		CO <sub>2</sub> /N <sub>2</sub>		CO <sub>2</sub> Qst	T <sub>dec</sub> (°C)	H <sub>2</sub> uptake mmol/g	References
		273K	298K	273K	298K				
TPP-1-NH <sub>2</sub>	554	4.1	2.60	43.6	33.1	41	--	--	He et al., 2014 <sup>1</sup>
TPP-1	863	3.4	2.10	53	35.6	31	--	--	He et al., 2015 <sup>1</sup>
TPP-2	525	2	1.10	22.7	15.1	27	--	--	He et al., 2015 <sup>1</sup>
TPP-3	785	3.2	2.20	28.1	22.3	26	--	--	He et al., 2015 <sup>1</sup>
TPP-4	140	2.6	1.80	50.4	42.5	26	--	--	He et al., 2015 <sup>1</sup>
TMPT	1640	6.02	--	--	--	38.4	<175	8.70	Lui and Zhang, 2013 <sup>2</sup>
TMP	1203	4.48	--	--	--	--	<300	8.20	Lui and Zhang, 2013 <sup>2</sup>
PAF-1	5341	2.05	--	--	--	--	--	8.30	Ben et al., 2012 <sup>3</sup>
JUC-Z8	4743	3.35	--	--	--	--	>430	10.94	Pei et al., 2014 <sup>4</sup>
JUC-Z9	4053	3.44	--	--	--	--	>430	10.89	Pei et al., 2014 <sup>4</sup>
HTP-A	569	1.14	0.68	11	--	24	--	3.20	Zhang et al., 2016 <sup>5</sup>
HTP-B	914	2.34	1.36	16	--	26	--	5.45	Zhang et al., 2016 <sup>5</sup>
STPI-1	4	0.42	--	37	--	31	--	--	Zhang et al., 2014 <sup>6</sup>
STPI-2	541	3.32	--	107	--	36	--	--	Zhang et al., 2014 <sup>6</sup>
STPI-3	378	2.51	--	71	--	28	--	--	Zhang et al., 2014 <sup>6</sup>
Td_PPI	2213	--	--	--	<30	--	--	8.00	Rao et al. 2014 <sup>7</sup>
PPN 3	5323	--	--	--	--	--	--	7.90	Lu et al, 2010 <sup>8</sup>
PPN 101	1096	10.09	--	--	--	--	--	--	Zhang et al., 2014 <sup>9</sup>
CMP-1-(OH) <sub>2</sub>	1043	1.8	1.07	--	--	27.6	--	--	Dawson et al., 2011 <sup>10</sup>
BF	1022	2.69	1.46	43	41	42.4	--	--	Saleh et al., 2014 <sup>11</sup>
COF-102	3620	1.56	--	--	--	25	--	--	Furukawa et al., 2009 <sup>12</sup>
PECONF-3	851	3.5	2.73	77	41	24.8	--	--	Mohanty et al., 2011 <sup>13</sup>
HCP-E	1470	2.93	1.77	--	9.2	26	--	--	Dawson et al., 2011 <sup>14</sup>
Zeolites-13X	615.5	--	0.63	--	--	--	--	--	Klinthong et al., 2014 <sup>15</sup>
MOF-Cu <sub>3</sub> (BTC) <sub>2</sub>	933	--	2.77	--	20.81	--	--	--	Bian et al., 2014 <sup>16</sup>
PEI50%-KIT-6	86	--	1.97	--	--	--	--	--	Kim et al., 2008 <sup>17</sup>



**Instrumentation.** All infrared spectra were recorded using a Varian 670-IR FTIR spectrometer with a PIKE Gladi ATR spare part using a powder samples. Flash chromatography was performed on silica gel 60A (35-70 micron) chromatography grade (Fisher Scientific). All NMR spectra were recorded on a Bruker AVANCE-III 400 MHz spectrometer in a suitable solvent using tetramethylsilane as the internal standard. Chemical shifts ( $\delta$ ) are reported in ppm. Elemental analysis was carried out using a Perkin-Elmer 2400 CHN elemental analyzer. Thermogravimetric analysis (TGA) measurements were carried out under  $N_2$  atmosphere using a TGA Q5000. The analyses entailed a drying step at 100 °C for 30 minutes followed by a ramp of 3 °C/min to 800 °C. The BET surface area of the network was determined by  $N_2$  and Ar sorption at 77 K and 87 K, respectively, using a Micromeritics ASAP-2020 and 3FLEX. Powder sample (polyimide network) was degassed under high vacuum at 120 °C for 15 hours prior to analysis. Analysis of the pore size distributions was performed using the NLDFT (Non-Local Density Functional Theory) model using  $N_2$  (at 77 K) and  $CO_2$  (at 273 K) sorption isotherms for carbon slit pore geometry provided by ASAP 2020 and the 3FLEX. Powder x-ray diffraction was performed a Bruker D8 Advance diffractometer with 0.02° per step and a scanning speed of 0.5 sec/step from 7 to 60°.

High pressure equilibrium measurements of  $H_2$ ,  $CH_4$ ,  $C_2H_4$  and  $C_3H_6$  were performed using a Rubotherm gravimetric-densimetric apparatus (Bochum, Germany) (Scheme S1), composed mainly of a magnetic suspension balance (MSB) and a network of valves, mass flow meters, and temperature and pressure sensors. The Rubotherm set-up is able to perform adsorption measurements across a wide pressure range (i.e., from 0 to 20 MPa). The adsorption temperature may also be controlled within the range of 77 K to 423 K. In a typical adsorption experiment, the adsorbent is precisely weighed and placed in a basket suspended by a permanent magnet through an electromagnet. The cell in which the basket is housed is then closed and vacuum or high pressure is applied. The gravimetric method allows the direct measurement of the reduced gas adsorbed amount ( $\Omega$ ). Correction for the buoyancy effect is required to determine the excess and absolute adsorbed amount using equations 1 and 2, where  $V_{\text{adsorbent}}$  and  $V_{\text{ss}}$  and  $V_{\text{adsorbed}}$  phase refer to the volume of the adsorbent, the volume of the suspension system, and the volume of the adsorbed phase, respectively.



**Scheme S1:** Representation of the Rubotherm gravimetric-densimetric apparatus

$$(1) \Omega = m_{absolute} - \rho_{gas} (V_{adsorbent} + V_{ss} + V_{adsorbed-phase})$$

$$(2) \Omega = m_{excess} - \rho_{gas} (V_{adsorbent} + V_{ss})$$

The buoyancy effect resulting from the adsorbed phase may be taken into account via correlation with the pore volume or with the theoretical density of the sample.

These volumes are determined using the helium isotherm method by assuming that helium penetrates in all open pores of the materials without being adsorbed. The density of the gas is determined using the Refprop equation of state (EOS) database and checked experimentally using a volume-calibrated titanium cylinder. By weighing this calibrated volume in the gas atmosphere, the local density of the gas is also determined. The pressure is measured using two Druck high-pressure transmitters ranging from 0.5 to 34 bar and 1 to 200 bar, respectively, and one low pressure transmitter ranging from 0 to 1 bar. Prior to each adsorption experiment, about 200 mg of sample is outgassed at 473 K at a residual pressure of 10<sup>-6</sup> mbar. The

temperature during adsorption measurements is held constant by using a thermostat-controlled circulating fluid.

## Materials

Veratrole, isobutyraldehyde, anthranilic acid, isopentyl nitrite, boron tribromide, 4,5-dichlorophthalonitrile, potassium hydroxide, acetic anhydride, isoquinoline, toluene, methanol (MeOH), potassium carbonate ( $K_2CO_3$ ), dichloromethane (DCM), tetrahydrofuran (THF), anhydrous dimethylformamide (DMF), hexane, acetonitrile, and chloroform ( $CHCl_3$ ) were purchased from Sigma-Aldrich and used as received. 2,3,5,6-tetramethyl-1,4-phenylene diamine (TMPD) was obtained from Aldrich and purified by sublimation prior to use. *m*-Cresol was distilled under reduced pressure and stored under nitrogen in the dark over 4 Å molecule sieves. 2,3,6,7,12,13-hexahydroxy-9,10-diisopropyltriptycenes was prepared according to the procedure described by Ghanem et al.<sup>18</sup>

## Synthesis of the trispthalonitrile (2)

Potassium carbonate (6.0 g, 49.59 mmol) was added to a stirred solution of 4,5-dichlorophthalonitrile (3.28 g, 16.6 mmol), 2,3,6,7,12,13-hexahydroxy-9,10-diisopropyltriptycene (2.4 g, 5.52 mmol), and anhydrous DMF (50 ml). After heating under argon atmosphere at 80 °C for 7 hours, the reaction mixture was added to 300 ml water. The resulting precipitate was collected by filtration, washed with water and methanol and dried to give (4.36 g, 98% yield). The crude product was purified by column chromatography over silica gel using DCM as eluent to give a white solid; (Found: C, 73.04 %; H, 3.54 %; N, 9.83 %. Calculated for  $C_{50}H_{26}N_6O_6$ : (C, 74.44% ; H, 3.25%; N, 10.42%). <sup>1</sup>H NMR (400 MHz, DMSO-*d*<sub>6</sub>, δ): 1.67-1.76 (m, 12H), 3.35-3.55 (m, 2H), 6.99-7.83 (m, 12H). FT-IR (powder, ν, cm<sup>-1</sup>): 3068-3113 (aromatic C-H), 2886-2977 (aliphatic C-H), 2236 (C≡N, str.), 1310 (C-O-C str.). HRMS (ESI): calc. for  $C_{50}H_{26}N_6O_6$  [M]<sup>+</sup>: 806.1914; Found 806.1886.

## Synthesis of 9, 10-diisopropyl trisanhydride monomer (3)

To a suspension of trispthalonitrile **2** (1.9 g, 2.36 mmol) in 25 ml ethanol was added a solution of potassium hydroxide (7.95 g, 69.5 mmol) in 25 ml of water. The reaction mixture was then refluxed with stirring for 20 h, and the hot solution was filtered to

remove any insoluble particles. After cooling, the filtrate was acidified by concentrated hydrochloric acid to pH 2-3. The resulting white precipitate was filtered off, washed with copious amount of cold water and dried in a vacuum oven at 60 °C to yield the hexacarboxylic acid as white solid (1.52 g, 70% yield), which was used in the following reaction without further purification.

To a round-bottom flask (50) ml fitted with a reflux condenser was added the hexacarboxylic acid (1.52 g, 1.4 mmol) and 20 ml of acetic anhydride. The reaction mixture was heated under reflux and argon atmosphere for 6 hours and cooled to 80 °C. The resulting yellow precipitate was filtered, washed with acetic anhydride and toluene and dried to give yellow powder (1.0 g, 83% yield). <sup>1</sup>H NMR (400 MHz, DMSO-*d*<sub>6</sub>, δ): 1.83-1.92 (m, 12H), 3.29-3.46 (m, 2H), 6.97-7.92 (m, 12H). FTIR (powder, ν, cm<sup>-1</sup>): 3040-30102 (aromatic C-H), 2806-2949 (aliphatic C-H), 1856 (asym. C=O), 1781 (sym.C=O), 1306 (C-O-C str). HRMS (ESI): calc. for C<sub>50</sub>H<sub>26</sub>O<sub>15</sub> [M]<sup>+</sup>: 866.1272; Found 866.1258.

### Synthesis of the polyimide network

To a dry Schlenk tube and under nitrogen flow were charged TMPD (0.142 g, 0.916 mmol), freshly distilled *m*-cresol (5 ml). After stirring under nitrogen flow for 5 minutes, an equimolar amount of the trisanhydride **3** (0.5 g, 0.611 mmol) was added in small portions. The reaction mixture was stirred at 0-5 °C for 15 minutes and the temperature was raised to room temperature and kept at that temperature for 7 h. Several drops of isoquinoline were added as a catalyst and the temperature was increased to 30 °C for 1 h, 80 °C for 0.5 h. After the gel was obtained 3 ml of *m*-cresol were added to the reaction mixture and the temperature was increased to 180 °C for 10 h and 200 °C for 7 h. During the heating the water of the imidization was removed continuously with a stream of nitrogen. After the solution was allowed to cool to ambient temperature, it was diluted with 5ml of *m*-cresol and then slowly added to vigorously stirred methanol (150 ml) and the resulting polymer was collected by filtration, washed with methanol and dried. Purification was achieved by refluxing network polymer in methanol and tetrahydrofuran for 3 h. The desired pale yellow polymer was collected and dried in vacuum oven at 120°C for 20 h (95% yield). Elem. Anal. Calculated for (C<sub>65</sub>H<sub>44</sub>N<sub>3</sub>O<sub>12</sub>) (repeat unit): C, 73.72; H, 4.19; N, 3.97%.

Found: C, 71.31; H, 3.60; N, 3.30%. FTIR (powder,  $\nu$ ,  $\text{cm}^{-1}$ ): 1778 (asym C=O, str), 1717 (sym C=O, str), 1302 (C-O-C, str), 1345 (C-N, str). BET surface area =  $1120 \text{ m}^2 \text{ g}^{-1}$ , total pore volume =  $0.86 \text{ cm}^3 \text{ g}^{-1}$  (at  $P/P_0 = 0.95$ , Ar adsorption). TGA analysis: (Nitrogen), initial weight loss due to thermal degradation commences at  $T_d \sim 400 \text{ }^\circ\text{C}$ .

## References

- (1) Y. He, X. Zhu, Y. Li, C. Peng, J. Hu, and H. Liu, *Microporous and Mesoporous Materials*, 2015, **214**, 181-187.
- (2) J. Liu and C. Zhang, *Macro. Rapid Comm.*, 2013, **34**, 1833-1837.
- (3) T. Ben, Y. Li, L. Zhu, D. Zhang, D. Cao, Z. Xiang, X. Yao, S. Qiu. *Energy & Environ. Sci.*, 2012, **5**, 8370-8376.
- (4) C. Pei, T. Ben, Y. Lia and S. Qiu, *Chem. Commun.*, 2014, **50**, 6134-6136.
- (5) C. Zhang, P. Zhu, L. Tan, L. Luo, Y. Liu, J. Liu, S. Ding, B. Tan, X. Yang, H. Xu, *Polymer*, 2016 **82**, 100-104.
- (6) C. Zhang, T. Zhai, J. Wang; J. Liu; B. Tan; X. Yang, H. Xu, *Polymer*, 2014, **55**, 3642-3647.
- (7) K. V. Rao, R. Haldar, C. Kulkarni, T. K. Maji and S. J. George, *Polymer*, 2014, **55**, 1452-1458.
- (8) W. Lu, D. Yuan, D. Zhao, C. I. Schilling, O. Plietzsch, T. Muller, S. Bräse, J. Guenther, J. Bluemel, R. Krishna, Z. Li, and H.-C. Zhou, *Chem. Mater.* 2010, **22**, 5964-5972.
- (9) M. Zhang, Z. Perry, J. Park, H.-C. Zhou, *Polymer*, 2014, **55**, 335-339.
- (10) R. Dawson, D.J. Adams and A.I. Cooper. *Chem. Sci.*, 2011, **2**, 1173-1177.
- (11) M. Saleh, H.M. Lee, K.C. Kemp and K.S. Kim, *ACS Appl. Mater. Interfaces*, 2014, **6**, 7325-7333.
- (12) H. Furukawa and O.M. Yaghi, *J. Am. Chem. Soc.*, 2009, **131** (2009), 8875-8883.
- (13) P. Mohanty, L.D. Kull and K. Landskron, *Nat. Comm.*, 2011, **2**, 401-406.
- (14) R. Dawson, E. Stöckel, J.R. Holst, D.J. Adams and A.I. Cooper, *Energy Environ. Sci.*, 2011, **4**, 4239-4245.
- (15) W. Klinthong, C.-H. Huang and C.-S. Tan, *Microporous Mesoporous Mater.*, 2014, **197**, 278-287.
- (16) Z. Bian, X. Zhu, T. Jin, J. Gao, J. Hu and H. Liu, *Microporous Mesoporous Mater.*, 2014, **200**, 159-164.

- (17) S.-N. Kim, W.-J. Son, J.-S. Choi and W.-S. Ahn, *Microporous. Mesoporous Mater.*, 2008, **115**, 497-503.
- (18) B.S. Ghanem, M. Hashem, K. Harris, K. Msayib, P.M. Budd, N. Chaukura, D. Book, S. Tedds, A. Walton, and N.B. McKeown, *Macromolecules*, 2010, **43**, 5287-5294.